Electronic Supplementary Material (ESI) for Nanoscale.

Supporting information for:

Tailoring Carbon Nitride Properties and Photoactivity by Interfacial Engineering of Hydrogen-Bonded Frameworks

Susmita Dolai¥[a], Jesús Barrio¥ [a], Guiming Peng[a], Andrea Grafmüller[b] , Menny Shalom*[a]

a. Department of Chemistry and Ilse Katz Institute for Nanoscale Science and Technology, Ben-Gurion University of the Negev, Beer-Sheva 8410501, Israel. Email: mennysh@bgu.ac.il

b. Department of Theory and Bio-Systems, Max Planck Institute of Colloids and Interfaces, Research Campus Golm, Potsdam 14424, Germany.

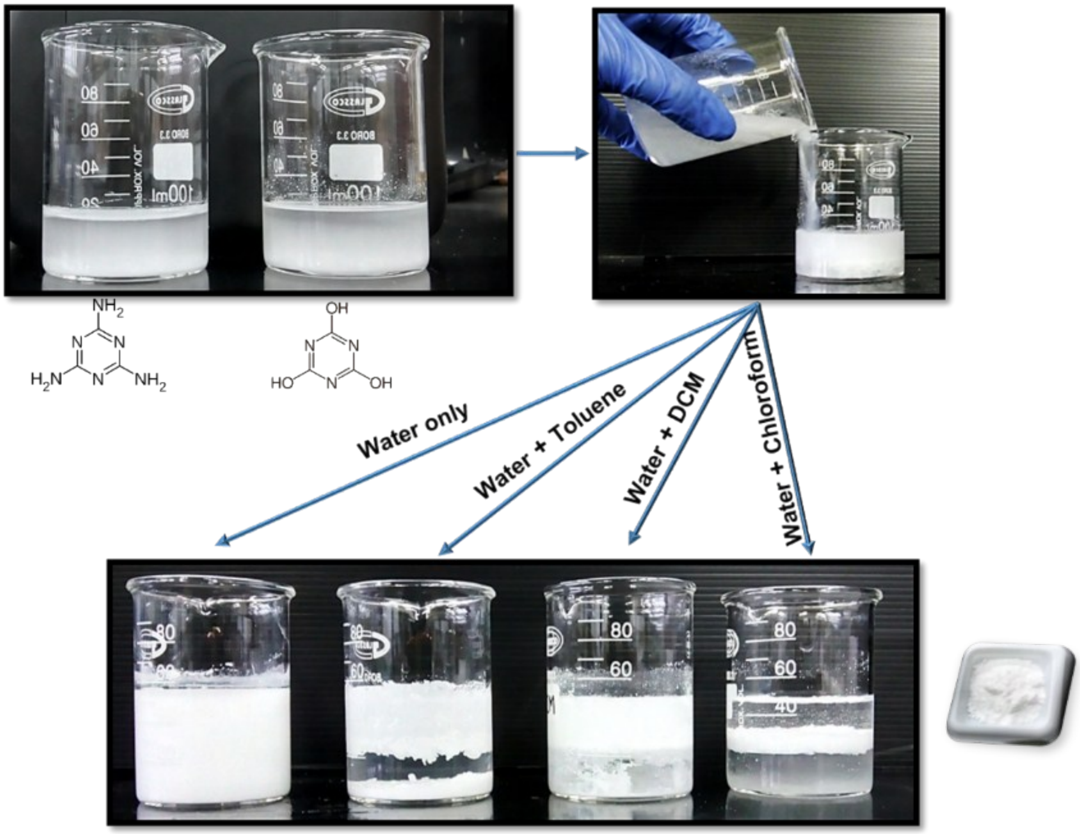

Scheme S1. Images of the synthesis of the CM supramolecular complexes in the interface between two solvents.

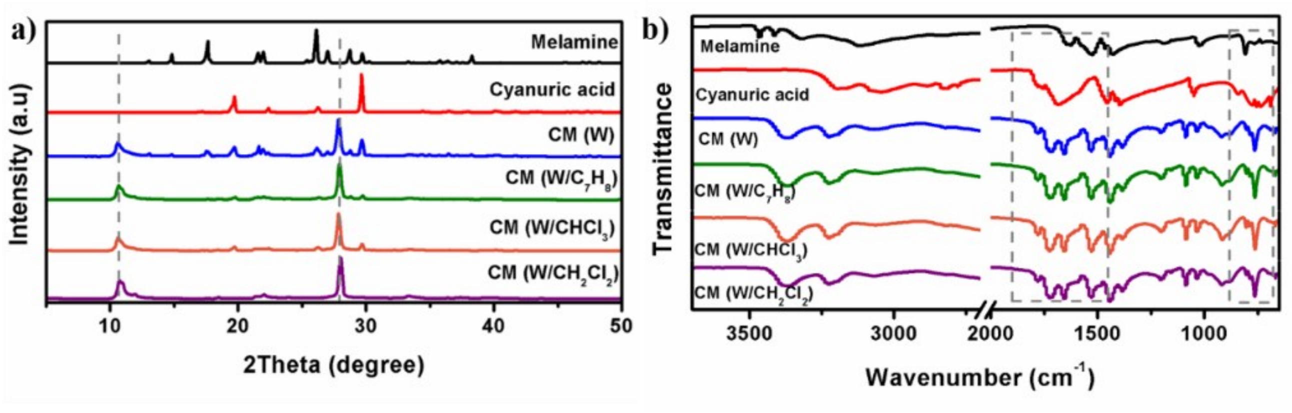

Figure S1. Characterization of supramolecular complexes synthetized in different solvents systems: (a) XRD, and (b) FTIR.

FTIR shows a general shift of the C=O stretching vibration of cyanuric acid, from 1600 to 1800 cm^{-1}, and the triazine ring vibrations from 814 to 734 cm^{-1} due to the hydrogen bond interaction.[1] XRD analysis shows two main peaks at 10.7° and 27.8°, which can be indexed as (100) and (002), corresponding to the in-planar packing and to a very well-developed lamellar stacking peak respectively.[2]

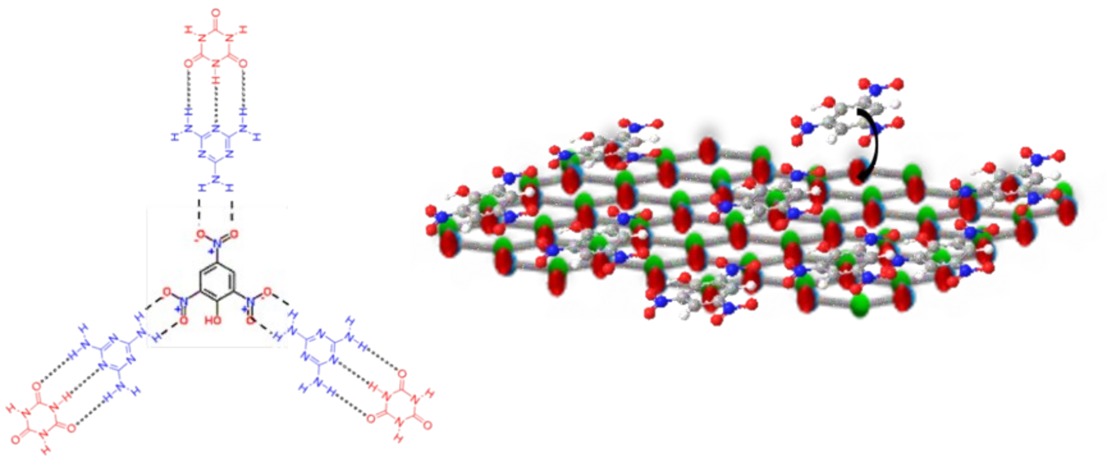

Figure S2. Proposed structure of the prepared assemblies after the incorporation of picric acid..

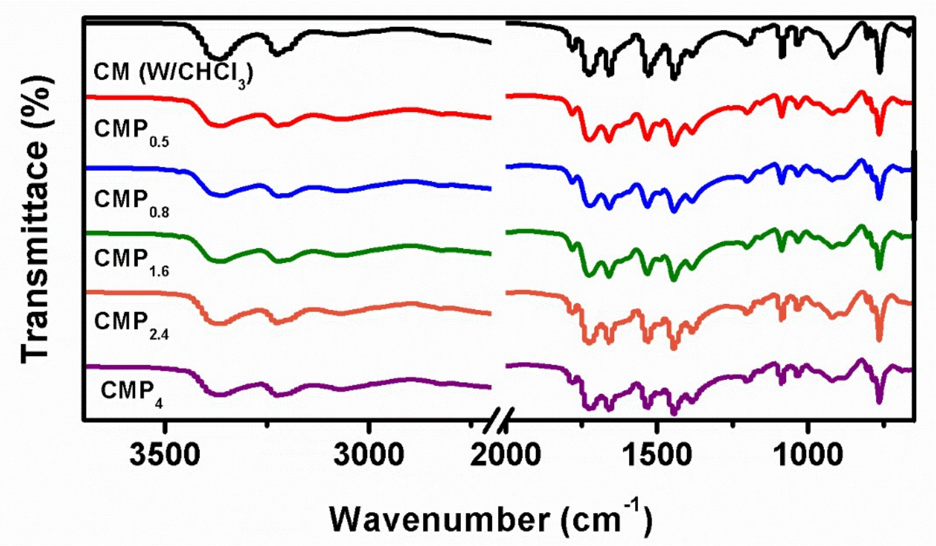

Figure S3. FTIR of CMP$_{x.}$ assemblies.

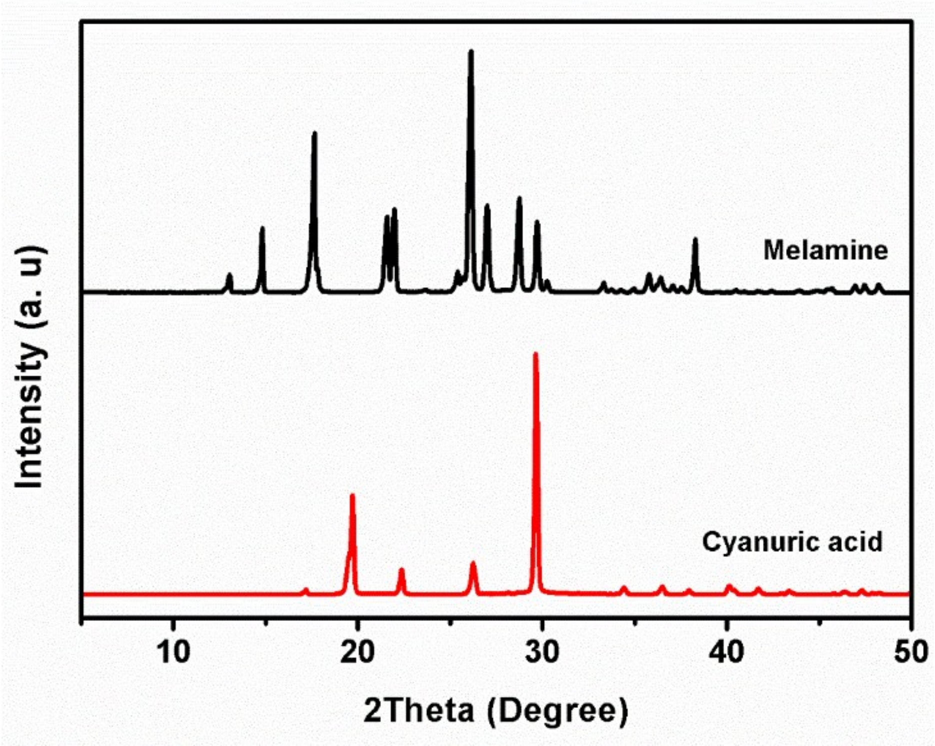

Figure S4. XRD patterns of melamine and cyanuric acid.

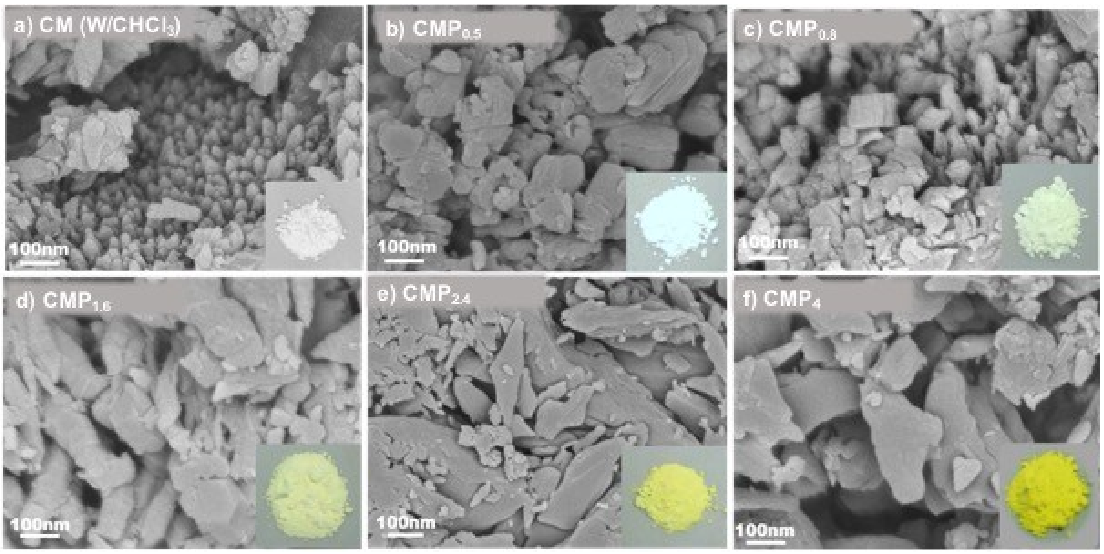

Figure S5. SEM images of CMP$_x$ complexes (insets: the corresponding digital images).

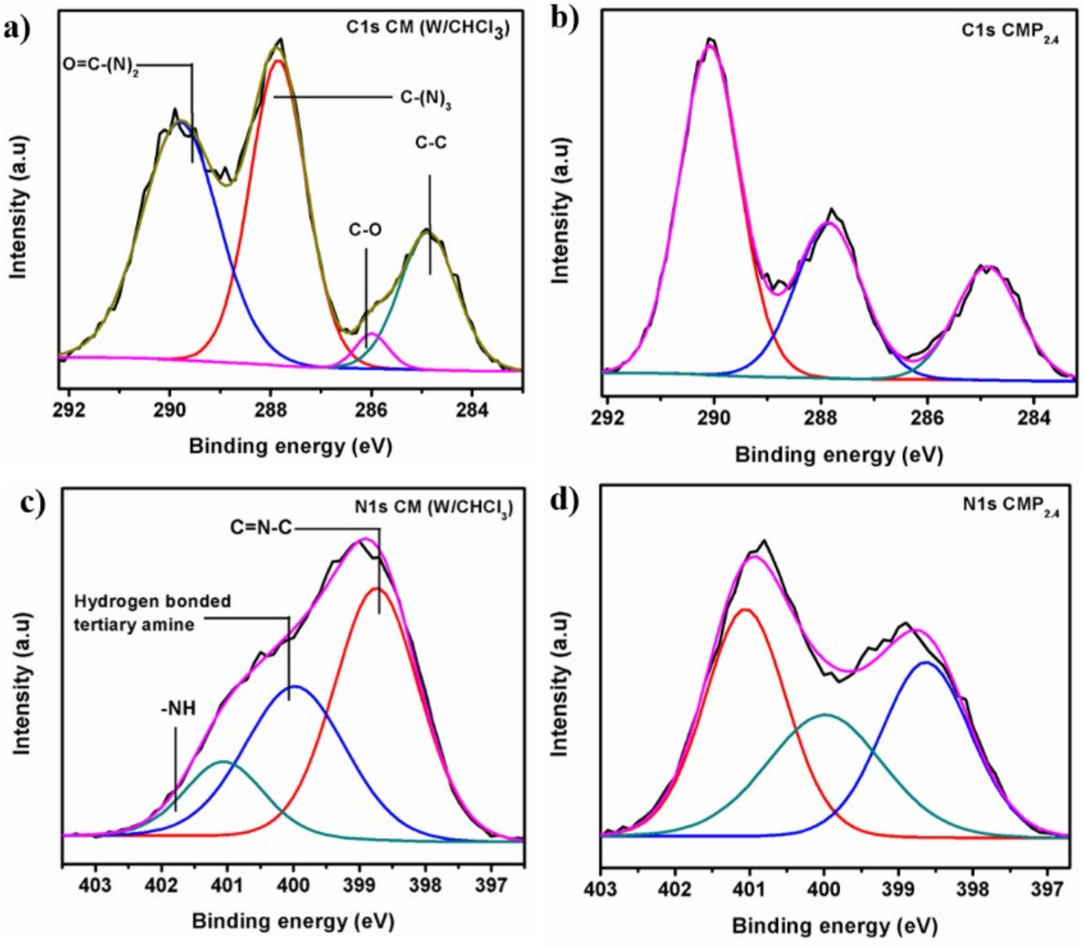

Figure S6. XPS spectra of CM (W/CHCl$_3$) and CMP$_{2.4}$ complexes.

The C1s XPS spectrum of CM (W/$CHCl_3$) shows four different chemical states at 284.8, 286.0, 287.8, and 289.7 eV, which correspond to C-C and C-O adventitious bonds, C-$(N)_3$ of melamine units, and O=C−$(N)_2$ of cyanuric acid, respectively. For $CMP_{2.4}$, the contribution at higher binding energies is shifted up to 290.1 eV and increased its atomic weight percentage, due to a synergistic contribution of O=C−$(N)_2$ of cyanuric acid and C-NO_2 from picric acid, while the remaining contributions are similar to the ones of CM (W/$CHCl_3$). The N1s spectra show 3 different contributions for both materials, which correspond to C=N-C coordination from the triazine units (at 398.7 eV), the tertiary amine (which performs hydrogen bonding with the OH units of cyanuric acid at 399.9 eV), and the remaining free amine groups (at 401 eV). It can be appreciated that the contribution of the free amine groups in $CMP_{2.4}$ becomes larger. We attribute this increase to the insertion and bonding of picric acid in the structure as it perturbs the NH-O hydrogen bonding between melamine and cyanuric acid, resulting in the release of melamine units.

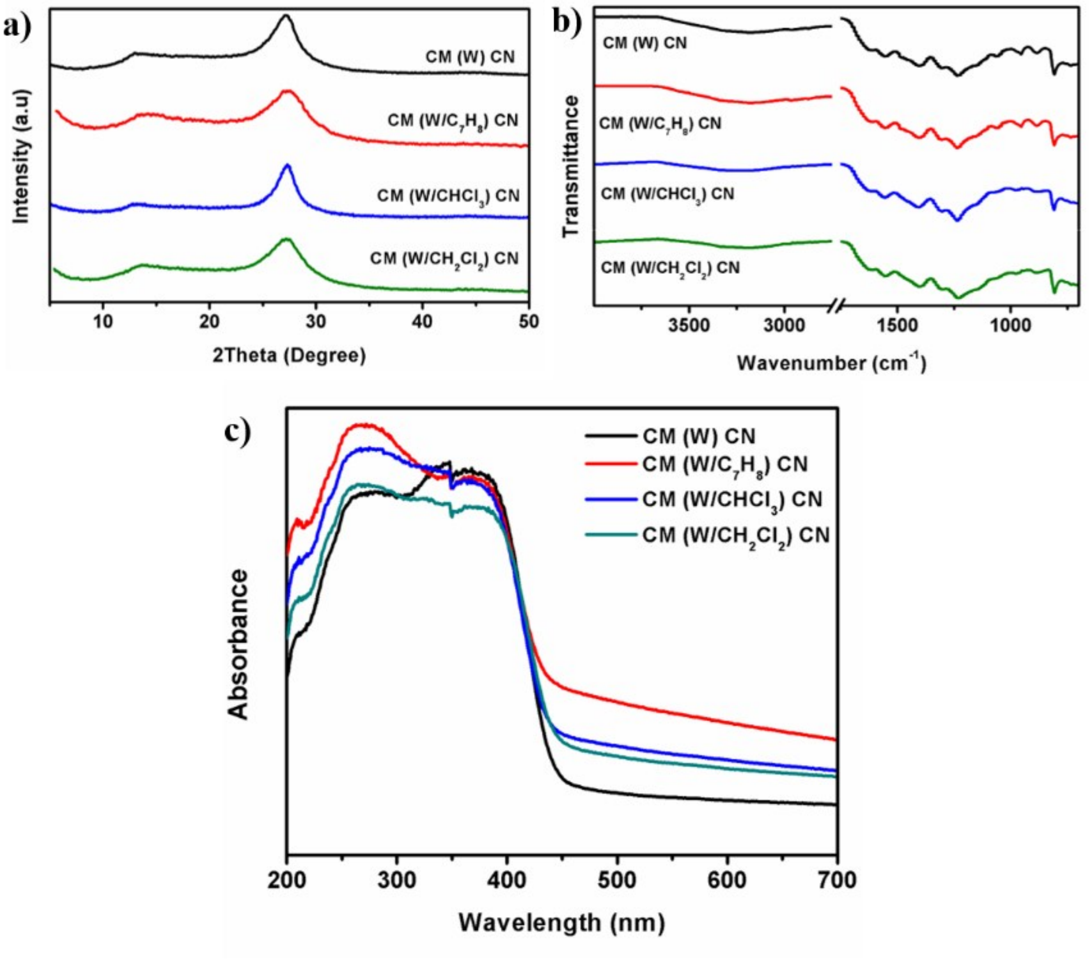

Figure S7. Characterization of CN materials prepared from CM: (a) XRD, (b) FTIR, and (c) UV-Vis.

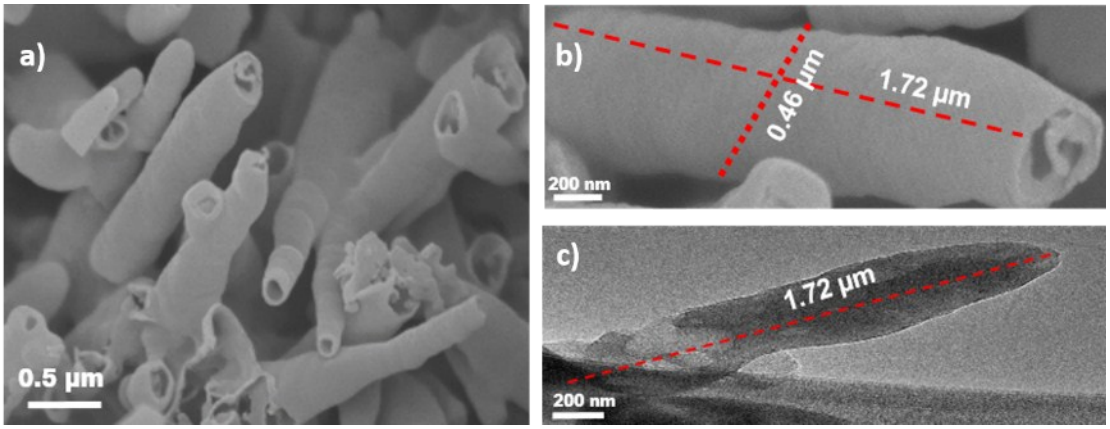

Figure S8. SEM (a and b), and TEM (c) of CM (W/$CHCl_3$) CN tube-like material.

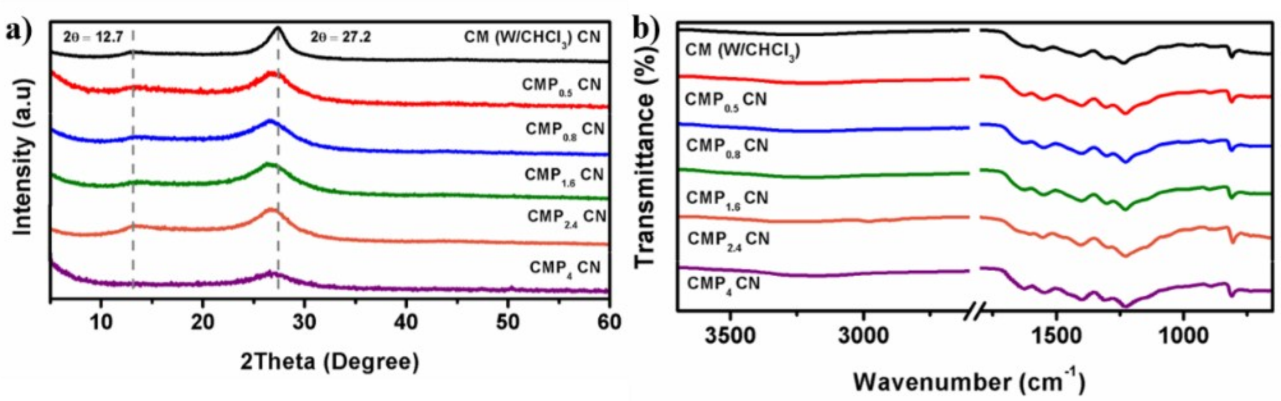

Figure S9. (a) XRD patterns, and (b) FTIR spectra of CN materials obtained after thermal condensation of CMP$_x$ assemblies.

The FTIR spectra shows the typical breathing mode of triazine units at 800 cm^{-1} and the stretching nodes of C-N heterocycles at 1200–1650 cm^{-1}. The XRD patterns display the diffraction peaks of CN-like materials. The interplanar stacking peak of aromatic systems at 27.2°, is slightly shifted to lower diffraction angles (26.6°) upon addition of picric acid. In addition, the in-plane peak at 12.7° corresponding to the (100) plane becomes less intense with higher amounts of picric acid and disappears in CMP$_{2.4}$ CN due to a feasible partial degradation of the tri-s-triazine units.

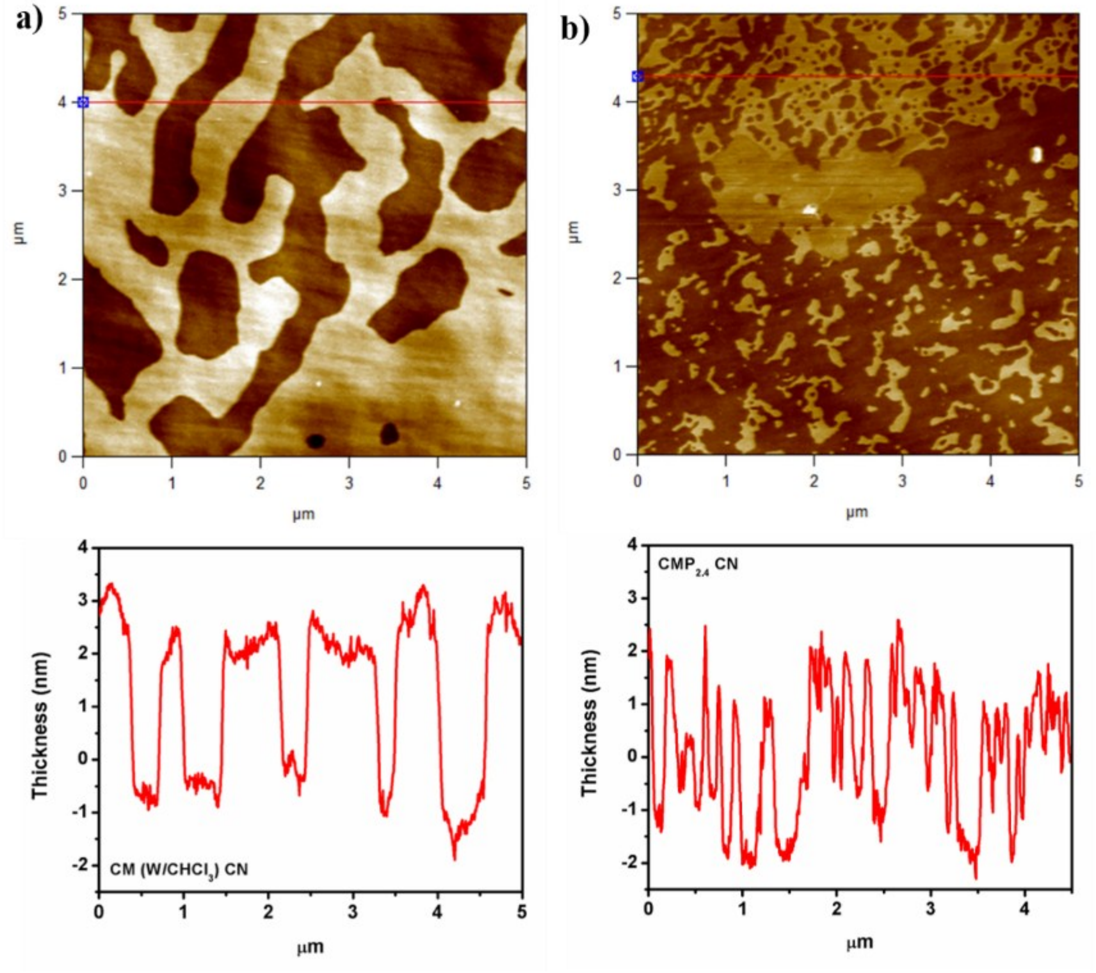

Figure S10. AFM images and the corresponding thickness plot (*z*-axis values at the linescan marked with a red line on the image) for (a) CM (W/CHCl$_3$), and (b) CMP$_{2.4}$ CN.

Table S1. Surface area analysis (BET model) of different carbon nitride materials.

Sample name	Surface area (m^2 g^{-1})
Melamine-CN	7.9
CM (W) CN	42.1
CM (W/CHCl$_3$) CN	54.1
CMP$_{0.5}$ CN	68.3
CMP$_{0.8}$ CN	71.5
CMP$_{1.6}$ CN	85.3
CMP$_{2.4}$ CN	92.0
CMP$_4$ CN	105.9

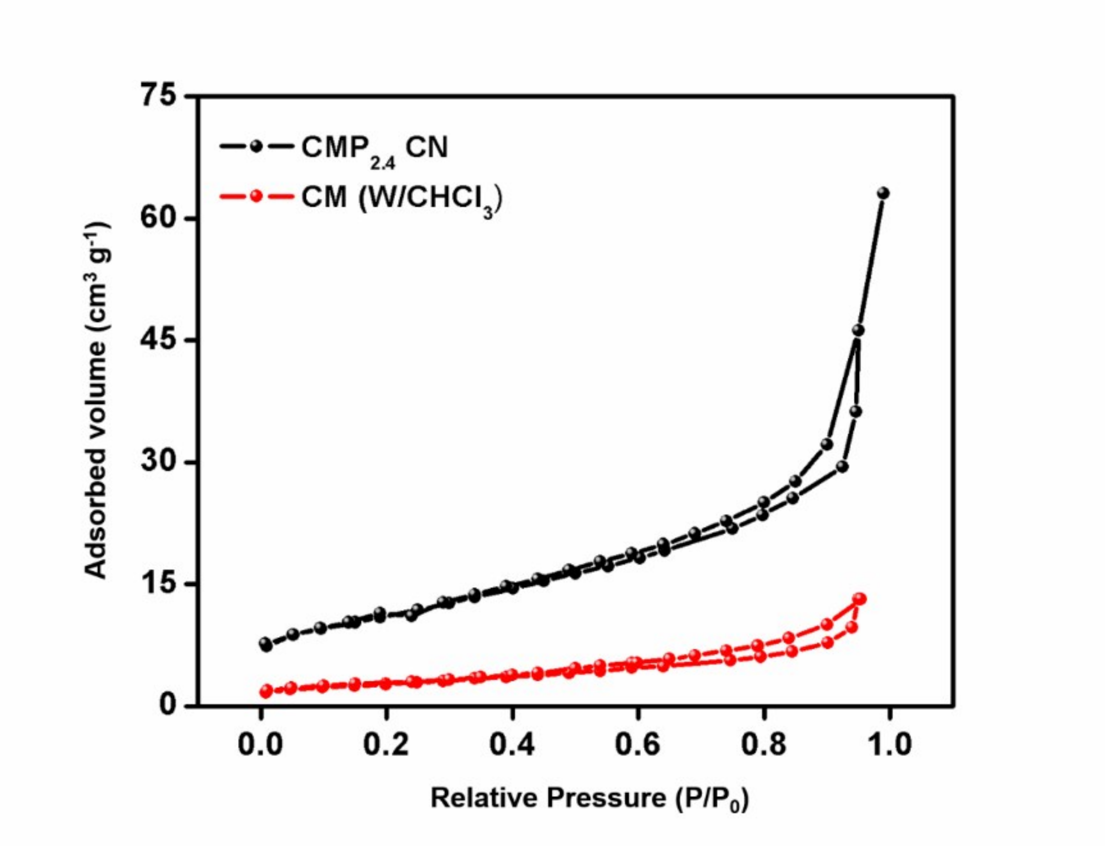

Figure S11. Nitrogen sorption isotherms of CM (W/$CHCl_3$) CN and $CMP_{2.4}$ CN.

Table S2. Elemental analysis (EA) data of carbon nitride materials.

Sample name	N (%)	C (%)	C/N ratio	H (%)
CM (W) CN	53.55	31.24	0.5838	2.30
CM (W/$CHCl_3$) CN	57.71	33.37	0.5782	1.79
$CMP_{0.5}$ CN	54.74	32.56	0.5948	1.86
$CMP_{0.8}$ CN	55.63	32.32	0.5856	1.78
$CMP_{1.6}$ CN	55.30	32.59	0.5893	1.85
$CMP_{2.4}$ CN	55.32	32.17	0.5815	2.26
CMP_4 CN	56.61	32.91	0.5864	1.62

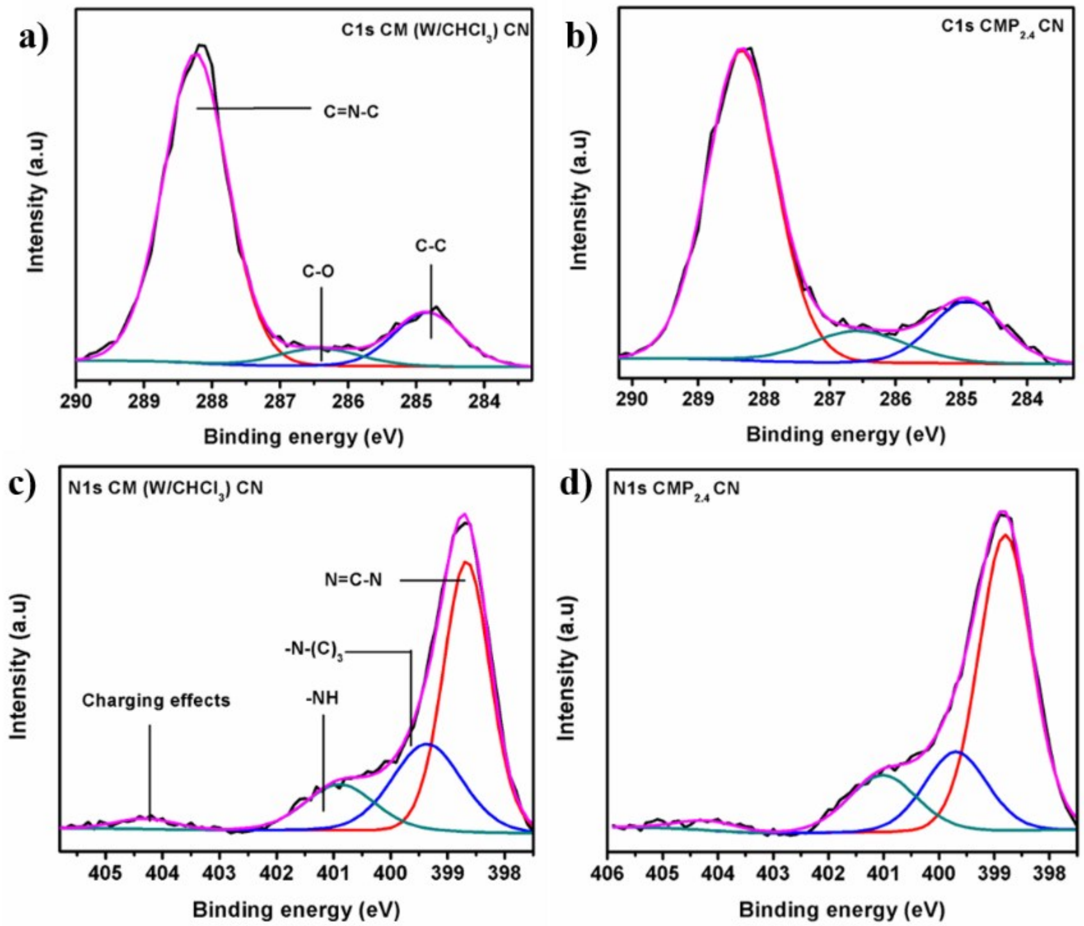

Figure S12. XPS spectra for C1s and N1s of CM (W/CHCl$_3$) CN and CMP$_{2.4}$ CN.

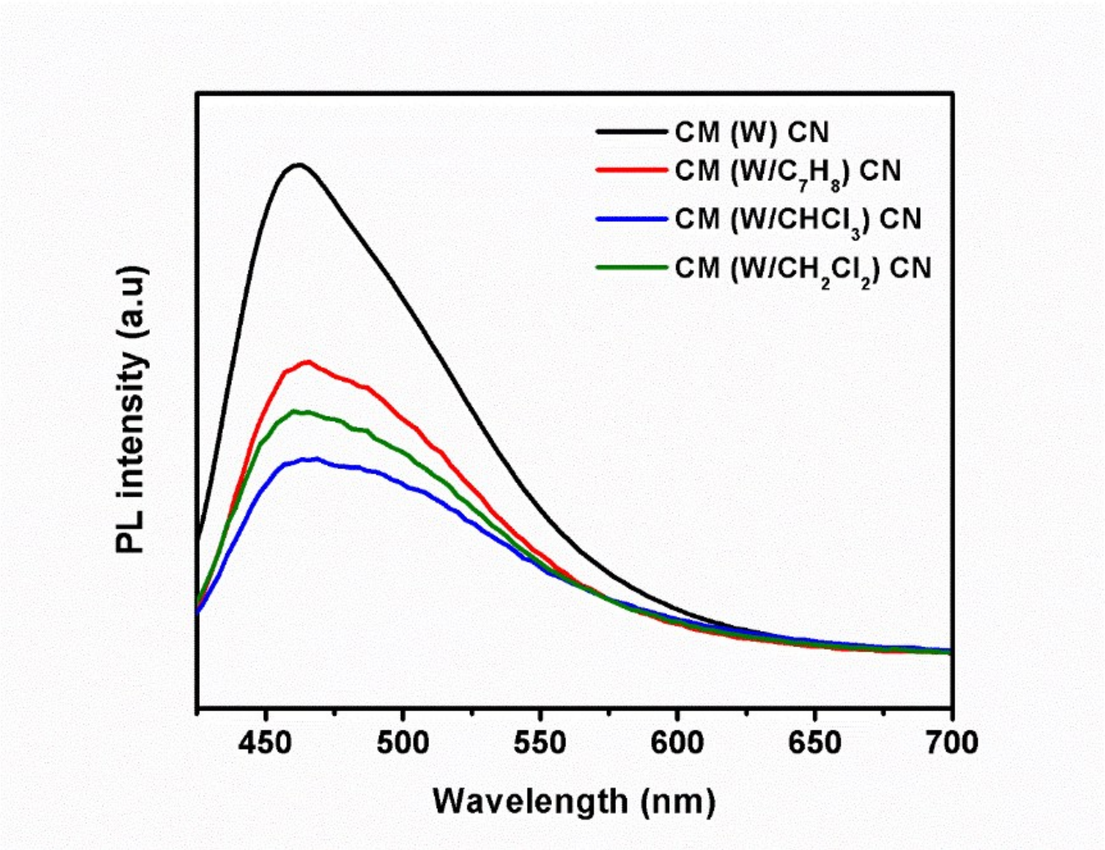

Figure S13. PL spectra of CM CN materials.

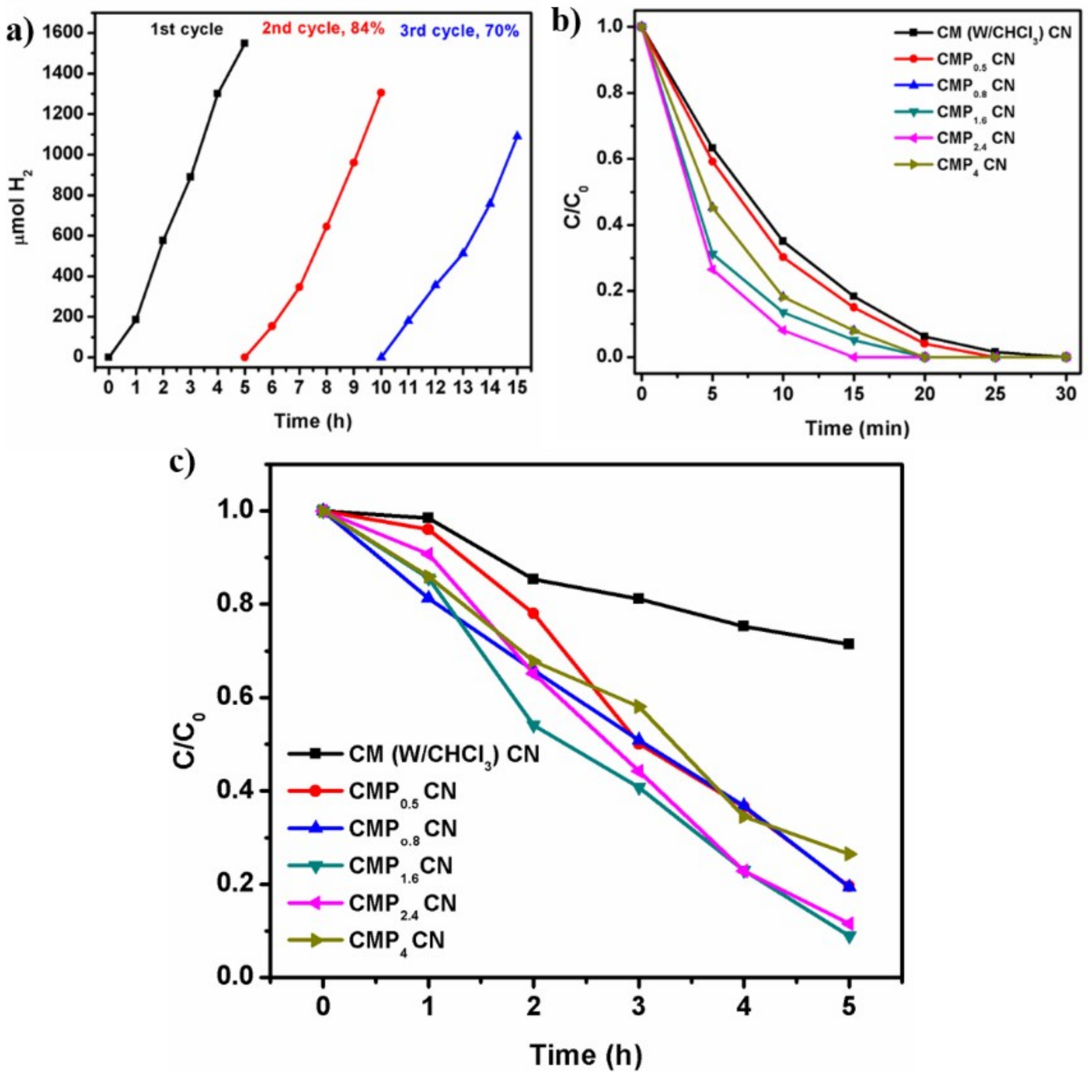

Figure S14. Photocatalytic performance characterization of various CMP$_x$-CN materials under visible light irradiation. (a) recycling performance of CMP$_{2.4}$ CN in hydrogen evolution reaction, (b) RhB photodegradation, (c) *p*-NP photodegradation.

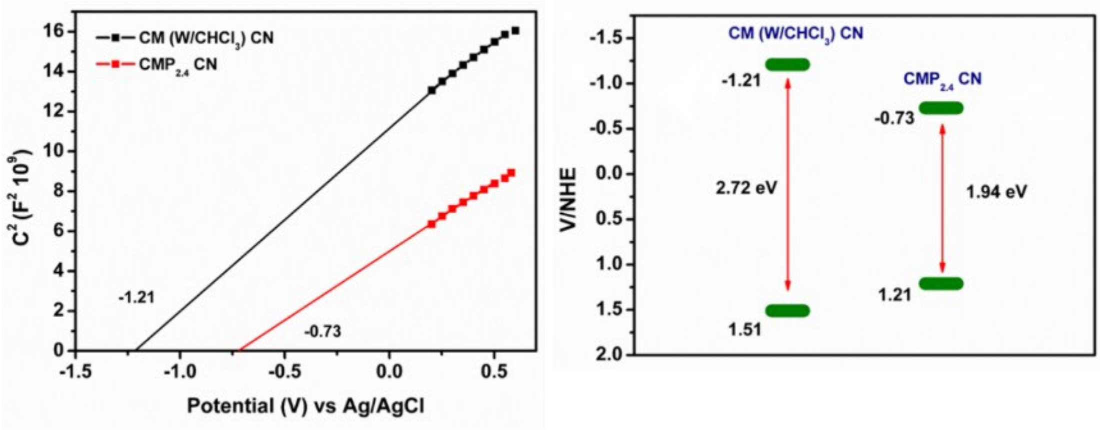

Figure S15. Mott Schottky measurements (a), and energy band structures (b) of CM (W/$CHCl_3$) CN and $CMP_{2.4}$ CN.

Supporting Information References:

[1] M. Shalom, S. Inal, C. Fettkenhauer, D. Neher, M. Antonietti, *J. Am. Chem. Soc.* **2013**, 135, 7118-7121.

[2] R. S. Bhosale, M. Al Kobaisi, S. V. Bhosale, S. Bhargava, S. V. Bhosale, *Sci. Rep.* **2015**, 5, 14609..